

# Micromotor grating optical switch

S. W. Smith, A. A. Yasseen, M. Mehregany, and F. L. Merat

*Electronics Design Center, Department of Electrical Engineering and Applied Physics,  
Case Western Reserve University, Cleveland, Ohio 44106*

Received February 14, 1995

We describe polysilicon micromotors with diffraction gratings fabricated on the polished surface of the polysilicon rotor for optical switching applications. The motors have rotor diameters of 0.5–2 mm with grating elements having periods of 1.80 and 3.86  $\mu\text{m}$ . These microswitches have rise times of 300  $\mu\text{s}$  and settling times of 500  $\mu\text{s}$  when driven by a 65-V switching pulse. The diffractive nature of the optical elements allows for multiple optical outputs from a single input beam. Both static and dynamic optical properties of the gratings are tested with a He–Ne laser at 633 nm. © 1995 Optical Society of America

Several schemes for light switching have been implemented, including deformable mirrors and liquid-crystal, electro-optical, and deformable grating optical modulators.<sup>1,2</sup> Each scheme has its advantages for particular applications, and most devices are limited to a single binary output. We recently presented diffraction grating scanners that use polysilicon micromotors whose rotors carry a reflective phase grating.<sup>3</sup> In this Letter we describe the use of these microscanners as a spatial light switch with multiple outputs for a single input. A schematic displaying the device operation is shown in Fig. 1.

The devices consist of polysilicon micromotors whose rotors have planar single or pyramidal (i.e., an element consisting of four pie-shaped regions adjacent regions having orthogonal line orientation) grating elements etched into the rotor with the grating spatial periods designed to be 2 and 4  $\mu\text{m}$ . These spatial periods are chosen to produce the largest possible angle between diffracted orders with the 1- $\mu\text{m}$  linewidths obtained from our photolithography process. The grating etch depth can be adjusted to distribute the optical intensity into a desired diffraction order from an incident light wavelength. Illuminated single-element gratings produce a row of diffracted orders perpendicular to the grating line pattern spaced at angles given by<sup>4</sup>

$$\theta_q = \theta_i + q\lambda/\Lambda, \quad q = 0, \pm 1, \pm 2, \dots,$$

where  $\theta_i$  is the angle of the incident beam relative to the normal,  $q$  is the diffraction order,  $\lambda$  is the wavelength of the incident light, and  $\Lambda$  is the grating period. As the motor rotates, the diffracted switched-beam  $k$  vector's components change by<sup>4</sup>

$$\begin{aligned} k_{dx} &= K \sin(\theta_r), \\ k_{dy} &= K \cos(\theta_r) - \sin(\theta_i), \\ k_{dz} &= \left(1 - k_{dx}^2 - k_{dy}^2\right)^{1/2}, \end{aligned}$$

where  $k_{dx}$ ,  $k_{dy}$ , and  $k_{dz}$  are components of the diffracted beam's  $k$  vector along the  $x$ ,  $y$ , and  $z$  axes, respectively,  $\theta_r$  is the rotation angle of the grating

diffraction grating in the  $x$ - $y$  plane (as shown in Fig. 1), and  $K$  is the ratio of the optical wavelength and the grating period,  $\lambda/\Lambda$ . A multifaceted pyramidal grating as described above can yield two perpendicular rows of diffraction orders. The grating scanners can operate in either transmission or reflection modes, thus allowing both in-line-fiber and free-space switches. Only reflection microswitches are considered in the Letter. Wobble and salient-pole micromotor<sup>5</sup> switches have been produced, but the focus of this Letter is on salient-pole micromotors, as they operate at higher speeds and have superior switch state repeatability in comparison with wobble micromotors. The microswitch motors have twelve stator poles that are separated into three phases (a phase is defined as a set of four stator poles separated by right angles). As the voltage step is applied to a phase of the salient-pole micromotor, the rotor is aligned parallel to that phase. This allows for three possible switch states for each row of diffraction orders.

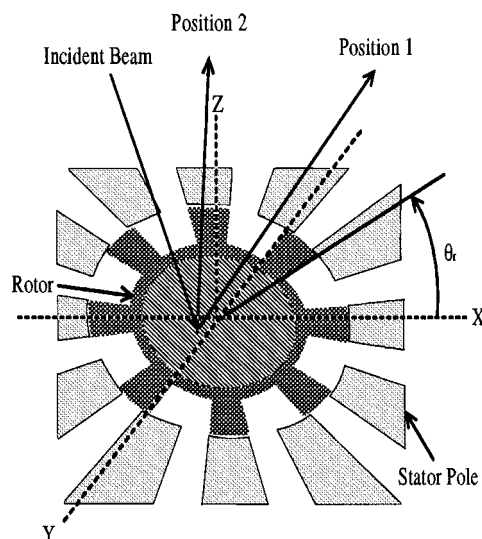


Fig. 1. Schematic of the operation of a salient-pole micromotor grating switch. As a voltage step is applied to a stator phase, the rotor aligns with that phase, causing diffracted orders to align with one of the three possible switch positions.

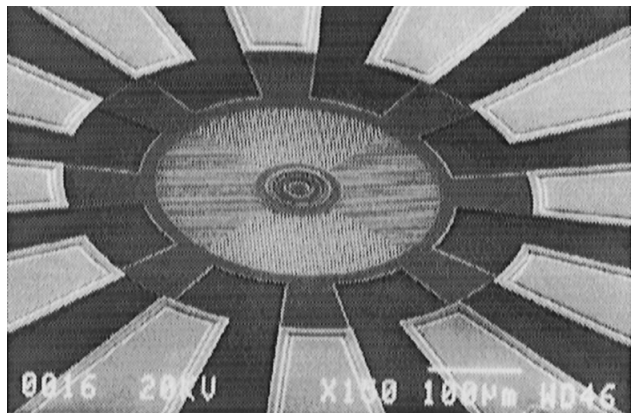


Fig. 2. Typical 500- $\mu\text{m}$ -diameter salient-pole micromotor scanner with polished polysilicon rotor and stator and pyramidal grating element of 1.80- $\mu\text{m}$  period.

The devices are fabricated<sup>3</sup> by initial deposition of a 450-nm layer of low-pressure chemical vapor deposition (LPCVD) silicon nitride for electrical isolation followed by 3.5  $\mu\text{m}$  of phosphosilicate glass for a sacrificial layer. The stator and the bearing post anchors are then patterned, followed by a 5.5- $\mu\text{m}$ -thick rotor/stator LPCVD polysilicon deposition and subsequent heavy doping with phosphorous. This polysilicon layer prevents the large-area rotors from warping out of plane. The rotor polysilicon layer, because of its thick, heavily doped nature, suffers from an inherent average surface roughness of 42 nm, which is unsuitable for optical applications. To eliminate this roughness, we polished the rotor polysilicon films after deposition and doping using chemical-mechanical polishing, which reduces the average surface roughness to 1.7 nm. Polishing not only improves the average surface roughness but significantly improves control of feature size definition and quality. After chemical-mechanical polishing of the rotor/stator polysilicon, the gratings are patterned and etched ( $\sim 0.5 \mu\text{m}$  deep) into the polysilicon layer with an isotropic dry etch to approximate a sinusoidal grating profile. The rotor/stator pattern is defined and delineated with a highly anisotropic dry etch to produce 1- $\mu\text{m}$  rotor/stator gaps. The flange mold is then defined and etched, followed by a 0.3- $\mu\text{m}$  bearing clearance oxidation. A 1.2- $\mu\text{m}$ -thick polysilicon layer is deposited by LPCVD and patterned to produce the bearing. Figure 2 shows a scanning-electron-microscope photograph of a typical diffraction grating micromotor switch with rotor/stator gap of 2  $\mu\text{m}$ .

The static optical characteristics of the diffraction grating were tested with a 633-nm He-Ne laser and a CCD camera. The grating periods of the nominally 2- and 4- $\mu\text{m}$  gratings were measured to be 1.80 and 3.86  $\mu\text{m}$ , respectively. These results are in close correspondence with the target design with the difference attributed to variations in timed etching and photolithography. The measured diffraction orders for the 1.80- $\mu\text{m}$  gratings are separated by  $20.79 \pm 0.62^\circ$ , and those for the 3.86- $\mu\text{m}$  gratings by  $9.8 \pm 53^\circ$ . Characterization of the diffracted laser beam profiles with a CCD camera shows that all diffraction

orders provide Gaussian beam profiles at distances of 10 cm to 1 m from the scanner. Gratings on polished polysilicon produce a higher degree of spatial uniformity and lower beam divergence than those on unpolished (see Fig. 3).

The overall diffracted efficiency of the grating is limited by the choice of polysilicon as the grating material because of its relatively low reflectance at 633-nm wavelength ( $\sim 30\%$ ). An average of 33.4% of the incident intensity is accounted for in the diffraction orders from all gratings tested.

The minimum operating voltage for tested salient-pole motors is as low as 45 V. As a 65-V step is applied to one of the motor stator poles, the rotor aligns with that pole with a rise time of 300  $\mu\text{s}$  and a settling time of 500  $\mu\text{s}$ . Typical data for angular displacement of the rotor as a function of time are shown in Fig. 4. The alignment time is dependent on the excitation voltage, with increasing voltage resulting in decreased switching times. The motor step transient speed is limited partly by viscous drag, and the switching speed can be increased by operation of the motor in vacuum, which can be accomplished by proper packaging. Results from our micromotor reliability studies have been published elsewhere.<sup>6,7</sup> Micromotors operated in a stepping mode (e.g., similar to a switching operation) have not failed in as many as  $3.6 \times 10^8$  start-stops, the limit of our experiments to this point.<sup>6</sup> In similar studies, micromotors whose bearings are coated with self-assembled monolayers have shown less than 4% performance variation over nine months.<sup>7</sup>

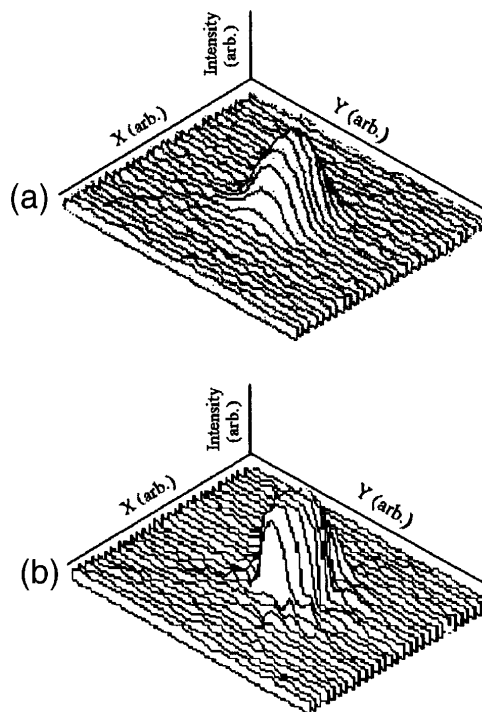


Fig. 3. Three-dimensional beam intensity profiles from similar gratings fabricated on (a) unpolished and (b) polished polysilicon rotors 0.5 m from a grating micromotor scanner by 633-nm light. Note the increased intensity and reduced beam divergence as a result of polishing.

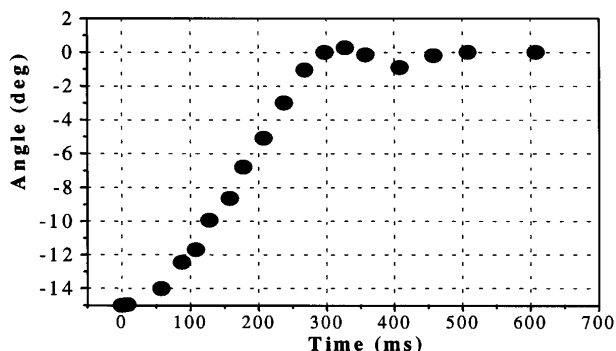


Fig. 4. Angular displacement of a microswitch rotor for a 65-V step excitation. Note the overshoot as the rotor aligns with the excited stator phase. Alignment with the excited stator phase is at 0°.

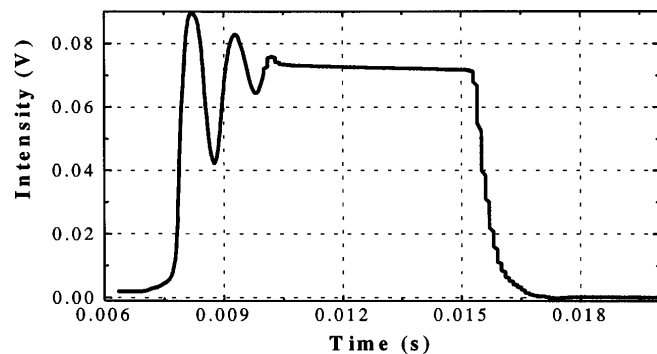


Fig. 5. Detector response to a beam diffracted from a rotating microswitch with a 65-V step excitation. Note the intensity variations caused by ringing of the rotor as it aligns with the excited stator phase.

Free-space switching was demonstrated with a 633-nm He-Ne laser normally incident upon a salient-pole single-element-grating  $1.80\text{-}\mu\text{m}$  microswitch. Spatial switching of a diffracted beam was examined with a silicon photodiode placed 10 cm from the microswitch surface and a dynamic digital signal analyzer. Figure 5 displays a typical detector response

to a beam diffracted from a rotating microswitch with switching pulse voltages of 80 and 120 V. Variation of less than 10% in optical intensity over hundreds of switch cycles was observed.

The micromotor grating optical switch introduced in this Letter benefits from planar silicon fabrication that is compatible with integrated-circuit processing. In addition, the microswitch has multiple diffraction order outputs for a single input, making the device attractive for multiplexers and computer interconnects in which multiple outputs from one input are desired. The combination of high-quality optical elements fabricated on micromotor rotors is established as a noteworthy competitor to many other schemes for spatial light switching.

The authors thank Girish Ramanathan of Case Western Reserve University for assistance in micromotor dynamical testing and Marcos Sorota of NASA Goddard Space Flight Center for suggestions on grating designs. This research was supported in part by the Advanced Projects Research Agency under contract F49620-94-C-0007 and by the National Science Foundation under grant ECS-9109343.

## References

1. O. Solgarrrd, E. S. A. Sadejas, and D. M. Bloom, *Opt. Lett.* **17**, 688 (1992).
2. Y.-L. Kok, *Opt. Eng.* **33**, 3604 (1994).
3. A. A. Yasseen, S. W. Smith, M. Mehregany, and F. L. Merat, in *Proceedings of IEEE Micro Electrical Mechanical Systems* (Institute of Electrical and Electronics Engineers, New York, 1995), pp. 175–180.
4. G. F. Marshall, eds., *Optical Scanning* (Dekker, New York, 1991), pp. 159, 242–244.
5. M. Mehregany, *IEEE Trans. Circuits Devices* **9**, 14 (1993).
6. M. Mehregany, S. D. Senturia, and J. H. Lang, *IEEE Trans. Electron Devices* **39**, 1136 (1992).
7. K. Deng, R. J. Collins, M. Mehregany, and C. N. Sukenik, *J. Electrochem. Soc.* **142**, 1278 (1995).